High Pressure Research
Vol. 28, No. 3, September 2008, 273–292

Taylor & Francis
Taylor & Francis Group

The COMPRES/GSECARS gas-loading system for diamond anvil cells at the Advanced Photon Source

Mark Rivers[a]*, Vitali B. Prakapenka[a], Atsushi Kubo[a], Clayton Pullins[a], Christopher M. Holl[b] and Steven D. Jacobsen[b]

[a] *Center for Advanced Radiation Sources, University of Chicago, Chicago, IL, USA;* [b] *Department of Earth and Planetary Sciences, Northwestern University, Evanston, IL, USA*

(*Received 28 February 2008; final version received 9 July 2008*)

We have designed and constructed a new system for loading gases at high pressure into diamond anvil cells at pressures up to 200 MPa. The gases are used either as quasi-hydrostatic pressure media surrounding the sample or as the sample itself. The diamond cell is sealed using a clamping mechanism, which permits nearly any type of diamond anvil cell to be used. Online ruby fluorescence and video imaging systems allow *in situ* monitoring of the pressure and gasket deformation as the cell is sealed, resulting in a very high success rate in loading cells. The system includes interlocks and computer control that allow it to be safely and easily operated by visiting users at the Advanced Photon Source. We present preliminary X-ray diffraction data on volume compression of single-crystal magnesium oxide (MgO) in helium up to 110 GPa.

Keywords: gas loading; high pressure; diamond anvil cell; X-ray diffraction; MgO

1. Introduction

Diamond anvil cells (DAC) are the most widely used devices for obtaining static high pressures above 3 GPa. In order to achieve quasi-hydrostatic conditions in the DAC at these pressures, it is necessary to use pressure media that are relatively soft solids. It is also desirable to use pressure media that are chemically inert, optically transparent, and weak X-ray scatterers. For DAC studies above about 10 GPa, rare gases are the preferred pressure media [1,2]. Argon can be loaded cryogenically, since it condenses above the temperature of liquid nitrogen. However, cryogenic loading has several disadvantages because the entire DAC is submerged in boiling liquid nitrogen, which can displace the sample. It is also difficult with Ar to control the initial pressure required to seal the cell, resulting in either failed loading or overshooting the desired initial pressure. Although helium and neon are preferred because of their lower X-ray scattering cross-sections and lower shear moduli, they cannot be loaded cryogenically at liquid nitrogen temperatures. Thus, it becomes necessary to load He, Ne, and other rare gases into the DAC

*Corresponding author. Email: rivers@cars.uchicago.edu

ISSN 0895-7959 print/ISSN 1477-2299 online

DOI: 10.1080/08957950802333593
http://www.informaworld.com

using high-pressure gas-loading techniques [3–6]. If the gas pressure is 100–200 MPa, then its density is comparable to the liquid at ambient pressure, and the DAC can be pressurized without excessive shrinking of the pressure chamber. High-pressure gas-loading also permits gas mixtures to be loaded, which generally cannot be done with cryogenic loading. Such systems operate by loading a DAC into a pressure vessel, pressurizing the vessel, and then remotely sealing the DAC, trapping the high-pressure gas with the sample inside the gasket hole between the two diamond anvils.

Noble gas pressure media, especially He or Ne, are particularly desirable for X-ray-based experiments (diffraction, emission spectroscopy, inelastic scattering, etc.) to minimize anisotropy in the stress field and to reduce the X-ray scattering background from the pressure medium. Because it is necessary to use high-intensity synchrotron radiation sources for high-pressure DAC experiments, it has become desirable to have a gas-loading system at a synchrotron beamline that is optimized for DAC studies. We have designed and built a new gas-loading system at GSECARS, sector 13 at the Advanced Photon Source, Argonne National Laboratory. Preliminary diffraction results are presented on volume compression of single-crystal magnesium oxide (MgO) in helium up to 110 GPa.

2. System design

2.1. *Design goals*

The APS and GSECARS are national user facilities for research using synchrotron radiation, hosting hundreds of high-pressure users from dozens of institutions. We wanted to build a system that could be safely and easily operated by our users with appropriate training. These scientists bring many different DAC designs to our beamlines. We therefore developed the following goals when designing our system:

- Ability to load many kinds of DACs. A closure mechanism (motor driven screws) closes a clamping device, which clamps the DAC closed. By not turning the tightening screws on the DAC directly, it is simple to accommodate different DAC designs. In many cases they just require different spacers, and in some cases a different clamp design. This design is inspired by the system described by Kenichi et al. [5].
- Optical access to view the cell while loading. This allows one to see when the diamonds contact the gasket as the cell is closed and to monitor gasket deformation. Optical access also allows *in situ* ruby fluorescence measurements for monitoring the pressure as the cell is closed. A similar optical access system, but without ruby fluorescence measurements, has been described by Couzinet et al. [6].
- Vacuum pump to clean the system before loading the gas and to save expensive gases by avoiding the need to purge the high-pressure system with gas.
- Ability to have no electrical parts except pressure transducers in the cabinet enclosing the high-pressure system. This allows flammable gas operation (*e.g.* hydrogen) in the future.
- Easy to safely operate. Use of air-driven valves, safety interlocks, and computer control.

2.2. *System components*

Based on these design goals, a system design was developed. The system layout is shown in Figure 1. A cross-section of the pressure vessel, with the cell clamp and the diamond anvil cell is shown in Figure 2. An annotated photograph of the system is shown in Figure 3. This design incorporates the following components:

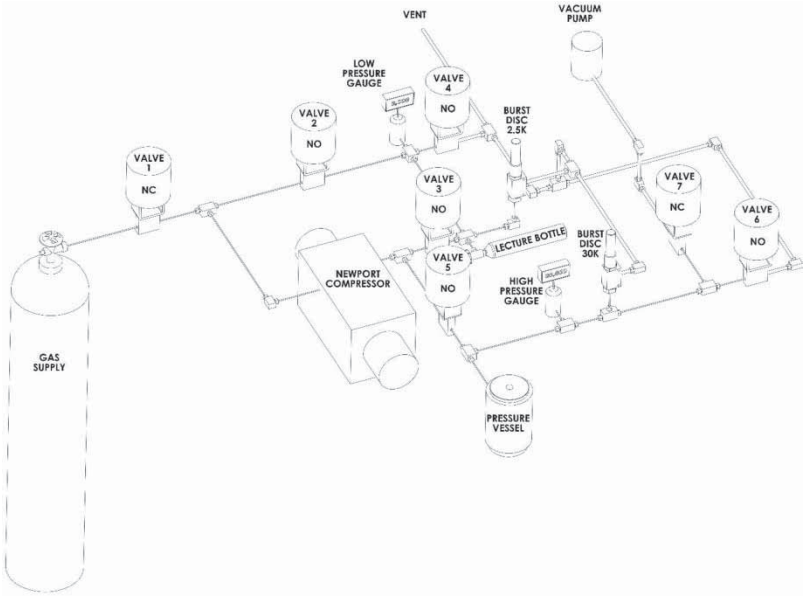

Figure 1. Schematic layout of the gas-loading system. Each valve is either normally open (NO), meaning it opens on loss of air pressure, or normally closed (NC), meaning it closes on loss of air pressure. The low-pressure burst disk (2.5 K) has a rating of 17.2 MPa (2500 PSI), and the high-pressure burst disk (30 K) has a rating of 207 MPa (30,000 PSI). There are six normal operational states of the system. In each state, all valves are closed, the compressor is off, and the manual valve on the lecture bottle is open unless otherwise noted. (1) Evacuating the system with the vacuum pump (valves 2, 3, 5, and 7 open, the manual valve on the lecture bottle closed), (2) filling the lecture bottle directly from the large gas bottle (valves 1, 2, 3, and 6 open), (3) filling the lecture bottle from the large gas bottle using the compressor (valves 1, 3, and 6 open, compressor on), (4) filling the pressure vessel from the lecture bottle (valves 2 and 5 open, compressor on), (5) venting the high-pressure system (valves 2, 3, and 6 open), (6) venting the low- and high-pressure systems (valves 2, 3, 4, 5, and 6 open, manual valve on the lecture bottle closed).

Low-pressure system. The low-pressure system includes valves 1, 2, and 4, a lecture bottle, a low-pressure gauge, and a 2.5 K burst disk. This part of the system operates at a maximum pressure of 13.8 MPa. It is isolated from the high-pressure system by valve 3.

High-pressure system. The high-pressure system includes valves 5, 6 and 7, a high-pressure vessel, a high-pressure gauge, and a 30 K burst disk. This part of the system operates at a maximum pressure of 207 MPa. It is isolated from the low-pressure system by valve 3.

High-pressure vessel. The pressure vessel (High Pressure Equipment Company, CL reactor) has a cloverleaf closure mechanism on each end plug, which works by rotating the plug 45° to lock and seat an O-ring seal. The upper end plug has a 25 mm thick sapphire window with a 12.5 mm optical aperture to allow viewing the diamond cell while it is being loaded. The lower end has two rotary feedthroughs to close the cell clamp. All components of the pressure vessel (cloverleaf closure mechanism, optical window, rotary feedthroughs) are commercial products and well-proven designs. The vessel has an outer diameter of 16.5 cm and an inner diameter of 7.62 cm, and it is made of 4340 alloy with hardness HB 311. The pressure chamber is 7.62 cm diameter and 8.89 cm tall. A detailed design of the vessel is shown in Figure 2. This vessel is not designed to load hydrogen, but a future more expensive system could use a hydrogen-safe alloy. The bottom plug is raised and lowered with pneumatic cylinders because the weight of the plug and the force required to seat the O-ring seal are too large for manual operation.

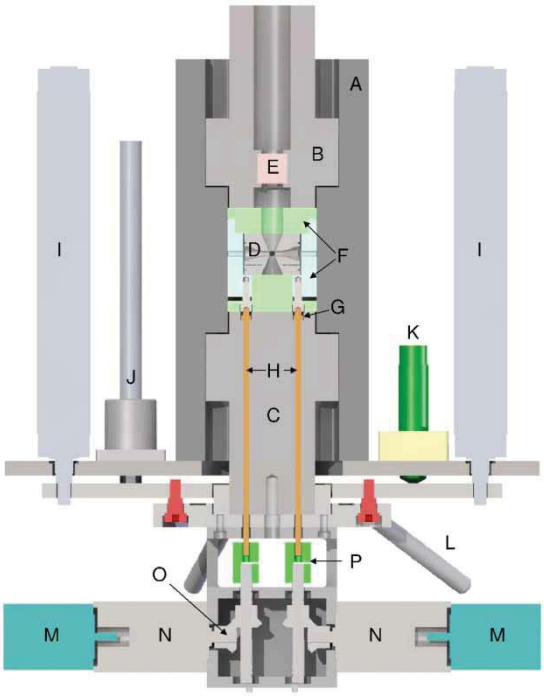

Figure 2. Cross-section view of the pressure vessel. (A) pressure vessel (outer diameter = 16.5 cm); (B) top end plug; (C) bottom end plug; (D) diamond anvil cell; (E) sapphire window; (F) cell clamp; (G) M6 screw; (H) rotary feedthrough; (I) pneumatic lifter; (J) guide bearing; (K) damper; (L) handle for rotating base assembly; (M) stepper motor; (N) gear reducer; (O) 90° gear; (P) coupling. The top and bottom end plugs are rotated 45° to seal using a cloverleaf closure. The base assembly (consisting of the bottom end plug, cell clamp with diamond anvil cell, stepper motors, and gears) is raised pneumatically and then rotated 45° to seal the pressure vessel. The damper slows the pneumatic lifter over the last 1 cm of travel, preventing sudden acceleration as the O-ring seal on the bottom end plug seats.

PLC. The operation of the air supply to the compressor and the air supply to all seven valves is controlled by a Programmable Logic Controller (PLC, Automation Direct Model DL205). The PLC ensures that valves are opened and closed in the correct sequence and ensures basic system safety. For example, it will open the vent valves before the burst disks fail and will turn off the compressor if the output pressure exceeds a maximum allowed value. The PLC inputs include the status of each valve and the cabinet door switches. The PLC outputs control compressed air solenoids to operate the valves and the compressor. It accepts requests over Ethernet from the control computer to operate the valves or the compressor. It sends the status of each of the valves over Ethernet to the control computer. The PLC controls the pneumatic cylinders that raise and lower the bottom plug of the pressure vessel. It also controls the laser interlock for the ruby fluorescence system. The PLC can be controlled and monitored from an Optimate panel on the front of the cabinet, or from the control computer. The operation of the PLC is discussed in detail in the Interlocks section below.

Compressor. The low- and high-pressure systems are pressurized with a dual-stage air-driven diaphragm compressor (Newport Scientific 46-14021-2) that can achieve 207 MPa output pressure. The diaphragm design ensures that there is no contamination of the gases being pressurized, and is safe for hydrogen operation.

Valves. There are seven high-pressure valves in the system (High Pressure Equipment Company). All are air-actuated and are driven via compressed air solenoids controlled by the PLC. A mix

Figure 3. Annotated photograph of the system. The four doors are open to show the interior of the cabinet. The control computer and the large gas cylinder are not shown.

of normally open (NO) and normally closed (NC) valves are used, so that the system fails into a completely depressurized state on loss of air pressure.

Gas cylinders. There are two gas cylinders in the system. The large gas cylinder is normally used as the supply of the pressurizing gas. The second is a small, lecture bottle (Linde Gas type A01) with a working pressure of 15.2 MPa, at which pressure it holds the equivalent of 1701 of gas at standard temperature and pressure (STP). The large gas cylinder is used only to fill the lecture bottle, either directly if the pressure in the large cylinder is >13.8 MPa or with the aid of the Newport compressor if the pressure is less than this. The high-pressure vessel is only loaded from the small lecture bottle, to limit the total volume of gas that can be pressurized to 200 MPa. This protects against excess stored energy in the system if users forget to load the cell clamp, DAC, or other components in the pressure vessel.

Burst disks. There are two burst disks in the system, which prevent over-pressurizing the low-pressure system and high-pressure system. The low-pressure system burst disk is rated at 17.2 MPa. The high-pressure system burst disk is rated at 207 MPa.

Pressure transducers. There are two pressure transducers in the system to measure the pressure in the low-pressure system and the high-pressure system. The transducers produce a 0–5 V output

over their full-scale pressure range. The low-pressure transducer (GP:50 Model 211-C-RT-7-FM) has a full-scale pressure range of 20.6 MPa. The high-pressure transducer (GP:50 Model 212-C-UC-AA) has a full-scale pressure range of 200 MPa.

Pressure meters. Each of the pressure transducers is connected to a digital panel meter (Omega DP41-S-S2AR). Each meter provides a digital panel display in pounds per square inch (PSI), 3 setpoint outputs that are connected to the PLC control system, and an RS-232 output that is connected to the control computer to read the actual pressure.

Vacuum pump and gauges. The entire system can be evacuated with a combination dry-roughing and turbomolecular vacuum pump (Alcatel Drytel 1025). This pump can achieve 10^{-6} torr. The pump is equipped with a combination Pirani and cold-cathode vacuum gauge (Alcatel ACC 1009) that can read from 1 atm to 10^{-9} torr. The gauge has an RS-232 interface to the control computer.

Optical system. There is a long-working distance objective, coaxial illuminator, and video camera system for observing the diamond cell through the optical window in the upper cloverleaf.

Ruby fluorescence system. An online ruby fluorescence system provides pressure measurement through the optical window in the upper cloverleaf end plug. The system consists of a Class IIIb green laser, a high resolution compact spectrometer, optical components (mirrors, splitters, lenses, etc.), a video camera, and a positioning system. This system is described in more detail below.

Control computer. There is a control computer running Microsoft Windows, which is the primary user interface to the gas-loading system. It displays the pressure in the low and high-pressure systems, the status of the compressor, and the status of all valves, sample image (picture-in-picture mode on a wide screen monitor), and ruby fluorescence system control. Users normally open and close the valves and operate the compressor though this computer, which sends requests to the PLC. The PLC is responsible for executing the operations if it is safe to do so. The control computer also operates the stepper motors to drive the cell closure mechanism and to position the laser optics. The control software is based on the EPICS control system, and the control screen for the system is shown in Figure 4. The only connection from the control computer to the system cabinet is an Ethernet cable. This would allow the control computer to be located remotely from the system if desired, for example, if the cabinet were to be in a separate room with no personnel access allowed during high-pressure loading.

Motor controller and driver. The diamond cell is closed via stepper motor driven rotary feedthroughs into the pressure vessel. A 4-channel stepper motor controller (ACS MCB-4B) is used to control and drive these motors and those for the visible light optics positioning. The controller is run by the control computer over an RS-232 connection.

Ethernet to serial converter. There are four RS-232 serial devices in the system: Omega pressure meters (two), vacuum gauge, and motor controller. A 4-port Ethernet to serial server (Moxa NPort 5410) is used to provide these serial ports.

Cabinet. The entire system except the control computer is mounted in a sturdy cabinet (from Item North America). The cabinet is shown in the photograph in Figure 3. The bottom level of the cabinet houses the compressor, vacuum pump, and valves. The upper left houses the lecture bottle, pressure vessel, and optical viewing system. The upper right side contains the controls and displays for the pressure gauges, vacuum gauge, and PLC. In the current design, there is electrical equipment in the same cabinet as the pressure vessel. In a future design for hydrogen operation, the

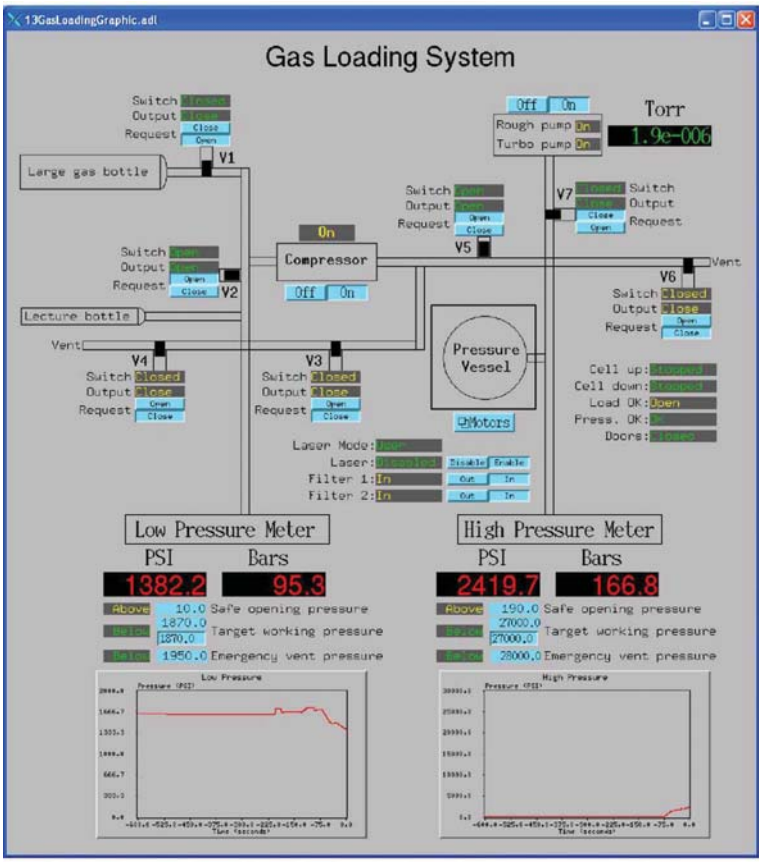

Figure 4. Computer control screen for controlling the system. The control system is based on EPICS running on the Microsoft Windows computer. It communicates with the Koyo PLC to receive status information and send requests to operate valves. RS-232 interfaces provide the pressure and vacuum information, and control the stepping motors to close the cell.

vacuum pump and all electronics could be mounted in a separate cabinet. The only connections to the gas-loading cabinet would be compressed air, vacuum, and the pressure transducer excitation and readout voltages.

The parts of the cabinet that contain high-pressure components (vessel, compressor, tubing, valves) are lined with 19 mm plywood panels. The part of the cabinet containing the pressure vessel has an additional shielding layer of 8 mm aluminum plate. This shielding is sufficient to protect the operators from plausible accidents, such as failure of a pressure fitting, breakage of the sapphire window, or ejection of a rotary feedthrough. The upper and lower cabinet doors have a sturdy latching mechanism, and the cabinet itself is of a strong aluminum frame construction. There are switches to sense that the enclosure doors are shut, and the safety system will not allow the high-pressure system to be pressurized when the doors are open. The upper left is also a laser enclosure for the ruby fluorescence system, and the doors must be closed before users can operate the laser.

2.3. *Safety features*

The primary hazard of any gas-loading system is the stored energy from the high-pressure gas. This hazard is minimized by keeping the total volume of the high-pressure gas as small as possible. The hazard is also mitigated through a set of engineered controls.

Lecture bottle

The stored energy in the system is controlled by the amount of gas that is compressed. The stored energy in the system is reduced by minimizing the empty volume (void spaces) in the high-pressure system. We have designed the diamond cell clamping device to minimize the amount of empty space. However, it is possible that an operator could forget to install one or more components in the pressure vessel (*e.g.* the diamond anvil cell or the clamping device), resulting in a much larger empty volume than normal. If the system were then pressurized from a large gas cylinder, the total amount of stored energy in the system would be much larger than desired. In order to protect against this, we have designed our system so that the high-pressure system can only by filled using a small 'lecture bottle' gas cylinder. With this protection, the total amount of gas that can be compressed to 200 MPa is small. If the user forgets to install space-filling components, then the compressor will simply empty the lecture bottle before the system reaches high pressure.

The amount of gas (at STP) in a standard size gas cylinder (*e.g.* Linde 044) at the standard fill pressure of 15 MPa is ∼6500 l. The amount of gas in a lecture bottle at 15 MPa (Linde size A01) is 170 l. We operate the lecture bottle at 13.8 MPa, so the gas volume is 155 l. We estimate the empty space in the system (pressure vessel, tubing, and valves) to be 60 cm^3. Assuming the ideal gas law is obeyed, the volume of gas required to reach 200 MPa from 0.1 MPa (room pressure) is $60\,cm^3 \times 2000 = 120\,l$. Thus, the lecture bottle with 155 l contains just over the amount of gas required to pressurize the system to 200 MPa. It is not possible to run the compressor with inlet pressure much less than 1.4 MPa, so this reserve capacity is needed.

Burst disks

The maximum allowed pressure in the low-pressure system is limited by the rating of the lecture bottle, which is 15.2 MPa working pressure, 25.5 MPa test pressure. The system contains a 17.2 MPa burst disk on the low-pressure system. This burst disk is connected to the system vent line and will vent the low-pressure system in the case of a malfunction that results in more than 17.2 MPa. The burst disk itself is a backup system. The primary protection is the low-pressure transducer, which is connected to an Omega meter with a low-pressure setpoint at 13.8 MPa. If the pressure exceeds this setpoint, then the PLC will open the low-pressure vent valve, V4.

The maximum allowed pressure in the high-pressure system is limited by the rating of the pressure vessel, which is 206.8 MPa. The system contains a 206.8 MPa burst disk on the high-pressure system. This burst disk is connected to the system vent line and will vent the high-pressure system in the case of a malfunction that results in >206.8 MPa. The burst disk is again a backup system. The primary protection is the high-pressure transducer, which is connected to an Omega meter with a high-pressure setpoint at 200 MPa. If the pressure exceeds this setpoint, then the PLC will open the high-pressure vent valve, V6.

Interlocks

The operation of the system is controlled via the PLC. All of the valves are air-operated, as is the compressor and the pneumatic cylinders that raise and lower the bottom plug of the pressure vessel. The PLC also implements the interlocks for the Class IIIb laser. Requests to the PLC to operate the valves and other components are made via the Optimate panel buttons mounted on the front of the cabinet or via the EPICS MEDM (Motif Editor and Display Manager) display on the control computer. The control computer communicates with the PLC via the Modbus protocol over Ethernet. The PLC will perform the requested action only if it is safe to do so. The actual state of the valves and other components is displayed on the Optimate panel and on the EPICS

MEDM display. The system will fail into a safe state, with the low-pressure and high-pressure systems vented and the compressor turned off, on failure of either electrical power or air pressure. This is achieved by using the correct combination of NO and NC closed high-pressure valves.

The PLC is programmed using ladder logic to implement the following interlock rules:

(1) If the Emergency Stop button is pressed, then put the system in a safe state, venting both the low-pressure and high-pressure systems. Close V1, open V2, close V3, open V4, open V5, open V6, close V7, turn off the compressor, and disable the laser.
(2) If the low-pressure system is above setpoint 3 on the low-pressure meter (13.8 MPa), then vent the low-pressure system. Open V4, close V1, close V3, and turn off the compressor. This is an emergency vent that should activate before the low-pressure burst disk fails.
(3) If the high-pressure system is above setpoint 3 on the high-pressure meter (200 MPa), then vent the high-pressure system and open V6. This is an emergency vent that should activate before the high-pressure burst disk fails.
(4) If the enclosure doors are not shut, then vent the high-pressure system (open V6). This protects personnel from being exposed to any components that are at pressures >13.8 MPa.
(5) If the lower plug of the pressure vessel is not in the closed position, then vent the high-pressure system. This prevents pressurizing the pressure vessel when the plug is not in the correct position.
(6) If both V3 and V5 are closed, then turn off the compressor. This prevents pressurizing the tubing between these valves, which would not be protected by a burst disk if both valves were closed.
(7) If the high-pressure system is above setpoint 2 on the high-pressure meter (normally 193 MPa), then turn off the compressor. This prevents over-pressurizing the high-pressure system without venting it.
(8) If the low-pressure system is above setpoint 2 on the low-pressure meter (normally 13.1 MPa) and V3 is open (so we are pressurizing the low-pressure system), then turn off the compressor. This prevents over-pressurizing the low-pressure system without venting it.
(9) If V6 is closed, then close V1. This rule has two effects:
    (a) Prevent pressurizing gas from the large gas cylinder directly into the pressure vessel. Only the lecture bottle can be the gas source for the pressure vessel.
    (b) Prevent refilling the lecture bottle if the high-pressure system is already pressurized.
(10) If the enclosure doors are open and the laser switch is not in Expert Mode (for alignment), then disable the laser. This prevents laser light from escaping from the enclosure.
(11) If the high-pressure system is above setpoint 1 of the high-pressure meter (normally 0.2 MPa), then close V7. This protects the vacuum pump from damaging high pressure.

3. Stored energy analysis

3.1. *Stored energy*

The ideal gas law can be written as $PV = nRT$, where P denotes pressure, V, volume, n, number of moles of gas, R, gas constant ($8.314\,\mathrm{m^3\,Pa\,K^{-1}\,mol^{-1}} = 8.314\,\mathrm{J\,K^{-1}\,mol^{-1}}$), and T, absolute temperature. At room pressure and 298 K the volume of a mol of an ideal gas is thus

$$V = \frac{nRT}{P} = \frac{8.314\,\mathrm{m^3\,Pa\,K^{-1}\,mol^{-1}} \times 298\,\mathrm{K} \times 1\,\mathrm{mol}}{101,325\,\mathrm{Pa}} = 24.45\,\mathrm{l}.$$

The ideal gas law predicts that pressure and volume are inversely proportional. At low pressure, nearly all gases follow the ideal gas law. At high pressure, real gases deviate from the ideal gas law

because the size occupied by the molecules themselves becomes comparable to the total volume occupied by the gases. Assuming ideal gas behavior will overestimate the stored energy in the system.

The energy of a material as pressure is increased at constant temperature is

$$E_2 = E_1 + \int_{p1}^{p2} V \, \mathrm{d}P$$

For an ideal gas, this becomes

$$E_2 = E_1 + nRT \ln\left(\frac{p_2}{p_1}\right)$$

The increase in energy as the pressure of 1 mol of gas is increased from 0.1 to 200 MPa at 298 K is thus

$$E_2 - E_1 = 1 \times 8.314 \times 298 \times \ln\left(\frac{200}{0.1}\right) = 18.8\,\mathrm{kJ}.$$

The volume of the lecture bottle is 155 l, which is thus $155/24.45 = 6.3$ mol. The stored energy in our system when it is pressurized to its maximum pressure is thus $18.8\,\mathrm{kJ} \times 6.3 = 118\,\mathrm{kJ}$. This energy can be compared with the muzzle energy of a 7.6 mm rifle bullet, which is about 3.5 kJ. So the stored energy is about 34 times greater than that of a rifle bullet. The energy can also be compared with that of a stick of dynamite, which is about 2500 kJ. So the stored energy is less than that in 1/20 of a stick of dynamite. Another comparison is with the stored energy in a standard gas cylinder, which contains about 6500 l of gas (at STP) at a pressure of 15 MPa. This is thus 266 mol of an ideal gas.

The energy content of the cylinder is thus

$$E_2 - E_1 = 266 \times 8.314 \times 298 \times \ln\left(\frac{15}{0.1}\right) = 3.30\,\mathrm{MJ}.$$

The stored energy of a standard gas cylinder is thus 28 times larger than the stored energy in our high-pressure system. The conclusion is that the stored energy is large enough to propel fragments with high velocity if there were to be a failure of a high-pressure fitting. We have placed the apparatus in a cabinet to shield against such hazards in the unlikely event of a failure. However, the energy is small when compared with that of standard compressed gas cylinders which are in routine use.

3.2. *Failure analysis*

3.2.1. *Velocity and energy of worst-case projectile*

If a part of the pressure vessel or other high-pressure component were to fail, it would cause one or more projectiles to be propelled at high speed. Here we consider what we believe to be a worst-case plausible scenario for such a failure. The velocity that a component would obtain is proportional to the force acting on it and the length of time that the force is applied. Components that are 'constrained' by being inside a tube (like the barrel of a gun) are accelerated for longer time before the gas can escape past them. In our system, the rotary feedthrough rods on the bottom plug of the vessel are the pieces that are most constrained in this manner, and hence are the 'worst-case' failure points.

These feedthrough rods have the following properties: material, stainless steel; length, 0.213 m; diameter, 0.00476 m; cross-section area, $1.78 \times 10^{-5}\,\mathrm{m}^2$; volume, $3.79 \times 10^{-6}\,\mathrm{m}^3 = 3.79\,\mathrm{cm}^3$; density, $8000\,\mathrm{kg/m}^3$; mass, 0.0303 kg.

The length of the hole in the pressure vessel plug is 0.173 m. If the rod were suddenly to lose all of the confining force which holds it in place, and has zero friction against being expelled from the vessel, it would accelerate for the time it takes to travel out of the pressure vessel plug, a distance of 0.173 m. The force acting on the rod is pressure times area. The maximum pressure is 200 MPa, or 2×10^8 Pa $= 2 \times 10^8$ kg m^{-1} s^{-2}. Multiplying by the cross-sectional area of the rod yields the force

$$2 \times 10^8 \,\mathrm{kg\,m^{-1}\,s^{-2}} \times 1.78 \times 10^{-5}\,\mathrm{m^2} = 3.56 \times 10^3\,\mathrm{kg\,m\,s^{-2}}.$$

We assume that the force is constant during this acceleration, because the increase in the volume of the gas (about 3.8 cm^3) as it ejects the rod is small when compared with the total gas volume estimated previously (60 cm^3). The acceleration will be force divided by mass:

$$\frac{3.56 \times 10^3\,\mathrm{kg\,m\,s^{-2}}}{0.0303\,\mathrm{kg}} = 1.17 \times 10^5\,\mathrm{m\,s^{-2}}.$$

The distance traveled in a given time at constant acceleration is $d = a \times t^2/2$, and the velocity as a function of time is $v = at$. Eliminating time (t) and solving for v yields

$$v = \sqrt{2da} = \sqrt{(2 \times 0.173\,\mathrm{m} \times 1.17 \times 10^5\,\mathrm{m\,s^{-2}})} = 201\,\mathrm{m/s}.$$

This predicts a velocity of 201 m/s, which is about three to five times less than the velocity of a rifle bullet.

The kinetic energy is

$$\frac{1}{2}mv^2 = \frac{1}{2} \times 0.0303\,\mathrm{kg}(201\,\mathrm{m/s})^2 = 612\,\mathrm{J}.$$

This is about six to eight times less than a rifle bullet.

3.2.2. *Penetration depth of projectile in aluminum*

Given this analysis of velocity and kinetic energy, it is possible to estimate the penetration depth in the 8 mm aluminum shielding plates that line the cabinet around the pressure vessel. Tanaka et al. [28] measured penetration depths and crater volumes for steel projectiles impacting aluminum plates at projectile velocities from 500 to 1800 m/s. This is two and a half to nine times greater than the velocity estimated above. They give their results in terms of the normalized properties: d = diameter of equivalent sphere for same mass as the projectile; $P_\mathrm{n} = P/d$ (normalized penetration depth, P = actual penetration depth); $V_\mathrm{n} = V/c_\mathrm{L}$ (normalized impact velocity, V = actual velocity, c_L = longitudinal sound speed of aluminum target = 6100 m/s).

For our system, we determine the normalized projectile diameter from the known volume of the rod (3.79 cm^3). The equivalent diameter is thus 1.94 cm. The normalized impact velocity is

$$V_\mathrm{n} = \frac{201\,\mathrm{m/s}}{6100\,\mathrm{m/s}} = 0.033$$

Using Equation (4) from [28]

$$P_\mathrm{n} = 27.3 \times V_\mathrm{n}^{1.58} = 27.3(0.033)^{1.58} = 0.125.$$

Thus, their results predict a normalized penetration depth of 0.125. Multiplying by the equivalent projectile diameter (1.94 cm) yields 0.24 cm predicted penetration depth, or 2.4 mm. Since the

actual thickness of the aluminum shielding on our enclosure is 8 mm, we conclude that this is sufficient to stop the worst-case projectile. This analysis is conservative, since it neglects the additional shielding provided by the 19 mm of plywood on the top of aluminum. Note that we have not considered the sudden rupture of the entire pressure vessel or the ejection of an end-plug, because we believe the engineering design of the vessel is sufficiently conservative to make sure a failure extremely unlikely.

3.2.3. *Other safety issues*

We have also calculated the effect of a sudden venting of the lecture bottle inside the cabinet. This would result in overpressure of 45% above ambient. The door latches and hinges are strong enough to withstand the resulting force on the cabinet panels. We have also calculated that if the door were struck by the worst-case projectile and the latches failed, the door velocity would be about 0.3 m/s, which is slow enough to present no hazard.

4. Ruby fluorescence system

The main advantage of the GSECARS gas-loading system compared with other available gas-loading systems is the ability to directly observe the sample while sealing the DAC and to monitor the pressure *in situ* by measuring the wavelength shift of the luminescence line from tiny ruby balls (Al_2O_3 doped with Cr) placed in the pressure chamber of the DAC [7].

The schematic illustration of the optical system for sample imaging and laser-induced luminescence measurements is shown in Figure 5. The 532 nm diode-pumped laser (DL) beam reduced to ∼1 mm in diameter with aperture (A1) is guided to the sample position (D) with mirrors (M). The dichroic mirror (DM) is used to separate the laser light and the visible radiation coming from the sample for spectroscopic luminescence pressure measurements and sample imaging. A Mitutoyo

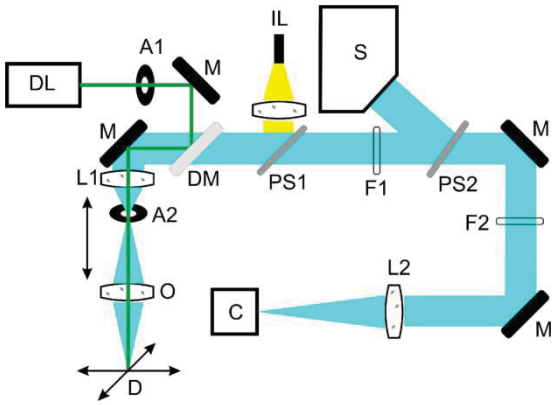

Figure 5. Schematic layout of the ruby fluorescence system optics for *in situ* video observation and pressure measurements in the gas-loading system. Main components: (DL) diode-pumped solid state 532 nm laser with adjustable power up to 100 mW (Lasermate); (S) high resolution spectrometer with direct-attached collimating lens (HR2000, Ocean Optics); (L1, L2) achromatic doublets with 75 and 400 mm focal length, respectively (Thorlabs); (O) 2× microscope objective with working distance 92 mm (Mitutoyo); (DM) 45 reflective green dichroic filter (Edmund); (IL) fiber illuminator with collimating lens; (A) adjustable aperture (Thorlabs); (BS) pellicle beamsplitter, 45/55% (Thorlabs), (M) silver coated mirrors (Thorlabs), (C) color CCD camera (Watec), (F1, F2) pneumatic driven longpass filters, cut-on wavelength 550 and 600 nm, respectively (Thorlabs), (D) diamond anvil cell position.

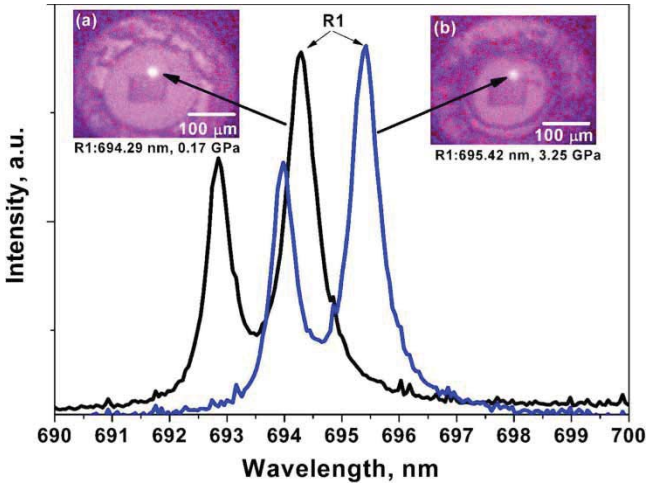

Figure 6. Typical spectrum of the ruby fluorescence in the DAC during gas-loading and corresponding images of the sample chamber in the DAC (inserts) inside the pressure vessel obtained through the 25 mm thick sapphire window. A ruby sphere is loaded in the cell along with a single-crystal sample, and the laser-induced fluorescence is visible through the color video camera in these images. The wavelength shift of the ruby fluorescence is used to measure the pressure in the DAC. (a) Before sealing the DAC with Ne gas pressure of 0.17 GPa. The clamp was then closed, increasing the pressure to 1.7 GPa (not shown). The cell and clamp were removed from the pressure vessel and the DAC screws were tightened. (b) The cell and clamp repositioned in the pressure vessel, pressure is now 3.25 GPa.

microscope objective (O) with magnification 2× and a relatively long working distance of 92 mm is used for sample imaging, laser focusing, and luminescence signal collection. Parallel light after the achromatic lens (L1, focal length of 75 mm) is directed to the high-resolution spectrometer (S) by pellicle beam splitter (PS2). The remaining transmitted light is focused on the CCD camera by achromatic lens (L2) with a focal length of 400 mm, providing total optical magnification onto the CCD chip of ∼10 times. We employ a confocal configuration in order to increase the spatial resolution and to eliminate parasitic luminescence from the 25 mm thick sapphire window located between the objective and the DAC. The variable confocal aperture (A2) placed in the focal plane of both the objective (O) and lens (L1) allows us to collect ruby luminescence from only the sample in the DAC. The high-resolution spectrometer (HR2000, Ocean Optics) has a holographic grating with a groove density of 1800, which covers the spectral range from 660 to 755 nm with an optical resolution of ∼0.1 nm. Motorized stages move the objective (O), confocal aperture (A2), and lens (L1) simultaneously along the vertical optical axis for precise focus adjustment without disturbing the alignment of the system. A high-performance large platform two-axis linear stage coupled with two stepper motor actuators moves the entire optical system in the horizontal plane to center the optics above the sample. A typical image of the laser-irradiated ruby ball in the DAC and the corresponding luminescence spectrum recorded with our system are shown in Figure 6.

5. Experience to date

The system has only recently received final safety approval for operation. We have now loaded more than 60 cells, with nearly 100% success rate. We have loaded two types of cells. The first is a symmetrical design, 48 mm diameter and 36 mm tall. The other is a 3-post design (43 mm diameter, 25 mm tall), using a simple cylindrical holder that fits inside the standard clamp shown

in Figure 2. The cells have been loaded with He or Ne at pressures of 15.8–17.9 MPa. The ability to measure the pressure as the stepper motors are driven to close the cell clamp has proved to be invaluable. The system does not need to be calibrated at all in order to close the cell and reach a desired pressure.

The basic sequence of operations to load a cell is as follows:

- The DAC is placed into the cell clamp, installing any filler pieces.
- The cell clamp is placed on the top of the bottom plug, aligning the hex socket screws to the rotary hex ends of the feedthroughs.
- The bottom plug and cell holder are raised in the pressure vessel by pressing the Cell Up button on the Optimate panel, raising the bottom plug with the air cylinders. Once the bottom plug is fully up, it is rotated 45° to the right to lock it into position and seal the O-ring seal. An interlocked pin is installed to ensure that the bottom plug is in the correct position and to prevent it from rotating.
- The doors to the enclosure are closed and the EPICS control screen is then used to close V6 and V7 and open V2, V3, and V5. This fills the pressure vessel from the lecture bottle. V3 is closed so that the compressor can pump the high-pressure system.
- The target working pressure for the high-pressure system is set to the desired value, up to a maximum of 29,000 PSI (200 MPa), and the compressor is started. It requires about 10 min for the compressor to pressurize the vessel to 180 MPa.
- Once the cell is pressurized, it is closed and sealed by rotating the stepper motors to drive the rotary feedthoughs clockwise, closing the cell clamp. The video system and ruby fluorescence systems are used to determine when the cell has sealed and reached the desired pressure.
- Once the cell has been closed and sealed, the pressure vessel is vented, optionally recapturing the gas into the lecture bottle.
- The DAC and clamp are removed from the vessel by lowering the bottom plug. The screws on the diamond cell itself are then tightened, using an Allen wrench that passes through access holes in the top of the cell clamp. Once these screws are tightened, the clamp and DAC are put back into the pressure vessel at room pressure, and the ruby luminescence system is used to verify that the pressure is now higher than it was with the clamp alone. If it is, then the operator can be sure that the DAC screws are now providing the confining pressure, and the cell clamp can be loosened and removed.

6. Application to equation-of-state studies

Equations of state relate thermodynamic system variables, principally pressure, volume, and temperature. Among many current problems in Earth and planetary science, solid-state chemistry, materials science, and condensed matter physics, there is a need for hydrostatic, or quasi-hydrostatic, compression of materials to a very high density. Isothermal equations of state are used as secondary pressure scales across the high-pressure sciences. Magnesium oxide (MgO) is stable to multi-megabar pressures with a $B1$ (NaCl) structure [8] and is among the most widely studied solid materials both as a pressure standard [9–11] and for testing new experimental methods and procedures [12–15], including first-principle calculations [16]. Here, we present preliminary X-ray diffraction data of single-crystal MgO to 110 GPa, about twice the pressure of previous compression studies carried out with helium pressure-transmitting media [9,10]. Detailed equation-of-state analysis will be presented elsewhere. Sample preparation and other experimental details are provided, including a comparison with non-hydrostatic compression of MgO in a solid KCl pressure medium.

6.1. *Sample preparation*

Single-crystal samples are often preferred for X-ray studies of diffracted intensities for structure refinements [17] as well as for equation-of-state studies because sharper peak widths and the greater number of reflections improve the precision of volume determinations [18]. Single-crystal samples 10–15 μm across and <10 μm thick are required for diamond-cell studies to Mbar pressures. Although crushing samples can produce fragments of suitable size, damage from crushing becomes obvious in single-crystal diffraction patterns, especially for materials such as MgO. Therefore, polishing is the preferred method of sample preparation.

In the current study, single-crystal MgO [1 0 0]-substrates measuring 10 × 10 × 0.5 mm were obtained commercially from MTI Corporation with >99.95% purity and sharp X-ray rocking curves. The 1 cm^2 platelet was ground from 0.5 mm thickness to ∼0.1 mm thickness using 3M™ Wetordry™ Tri-M-ite™ SiC paper with 600 ANSI grit (P1200 European grit). Subsequent polishing of the 10 × 10 mm plate to 50 μm thickness was carried out using a diamond-impregnated 3M™ lapping film, progressively from 9 to 3 μm, and finishing with 0.5 μm. The diamond film is stationary and set with a thin layer of water onto a thick glass plate of very high flatness while the sample is polished by hand. Samples are glued to frosted-glass petrographic slides, measuring 27 × 46 × 1.2 mm from Ward's Natural Science. We have found Loctite® 495 instant adhesive to be the best for holding samples to the slide in very-thin polishing applications. After polishing to 50 μm thickness, the sample becomes easy to cleave using a razor blade without significant damage. Cleavage fragments with lateral dimensions of 1 mm (maximum) or less are glued and polished to about 20 μm thickness using a 3-μm diamond film with water lubricant. We first place the crystals on the slide, and let Loctite® 495 run underneath the sample from the sides, forming a very thin bond between the frosted slide and the sample. Finally, a 3 μm or a 0.5 μm diamond film is used until the sample and glue are visibly about to peel away from the glass slide. Using the Loctite-495 adhesive and frosted slides, we have been able to polish MgO crystals μm down to 5–8 thick.

For helium loading, the diamond-cell gasket must have initial thickness and hole-diameter suitable to accommodate the high compressibility of helium [19]. In this experiment, a symmetrical piston—cylinder style diamond cell was used with beveled anvils having 100 μm inner and 300 μm outer culet diameters. Rhenium gaskets were prepared by pre-indenting with rubies and monitoring the fluorescence pressure to about 28 GPa. For this culet size, the initial gasket thickness was 25–30 μm. An EDM drill fitted with a stainless-steel acupuncture needle tool was used to erode the initial hole diameter of about 80 μm, illustrated by the white ring in Figure 7.

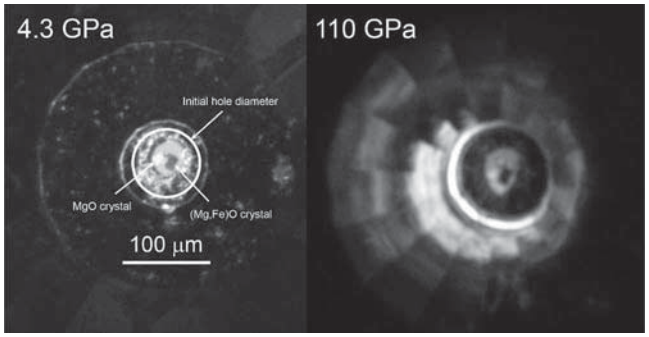

Figure 7. View into the diamond-anvil cell with single-crystal MgO after loading with helium at 160 MPa. The beveled anvils have 100-μm inner culet and 300-μm outer culet. The initial hole diameter, about 80 μm (white ring shown in the left panel), was reduced by about 40% on compression to 4.3 GPa. Subsequent compression to 110 GPa (right panel) did not change the hole diameter further by more than 10–15%. Gasket material is Re with initial thickness of 25–30 μm.

6.2. *Gas loading*

The MgO was loaded and sealed at about 160 MPa of He pressure using the gas-loading system. After compressing to 4.3 GPa, the hole diameter was reduced to about 40–50 μm diameter, shown in Figure 7. Thus, for a 25–30 μm initial gasket thickness and 100/300-μm inner/outer culet anvils, ∼40% shrinkage can be expected for helium loading at 160 MPa. The right panel of Figure 7 shows the sample chamber at 110 GPa. Thus, there was no significant shrinkage of the hole diameter after ∼5 GPa, and eventually the hole diameter enlarged slightly above about 90 GPa. Ultimately, a crack formed within the diamond at 115–120 GPa and the pressure immediately dropped back to about 90 GPa.

6.3. *Data collection*

Synchrotron X-ray diffraction data were collected on the 13-BMD beamline of GSECARS at the APS. A monochromatic X-ray beam with wavelength $\lambda = 0.2755$ Å (∼45 keV) was focused to about 5 × 13 μm spot size and used to obtain diffraction images from separate crystals, including MgO, in the diamond cell shown in Figure 7. Diffraction patterns were recorded on an MAR345

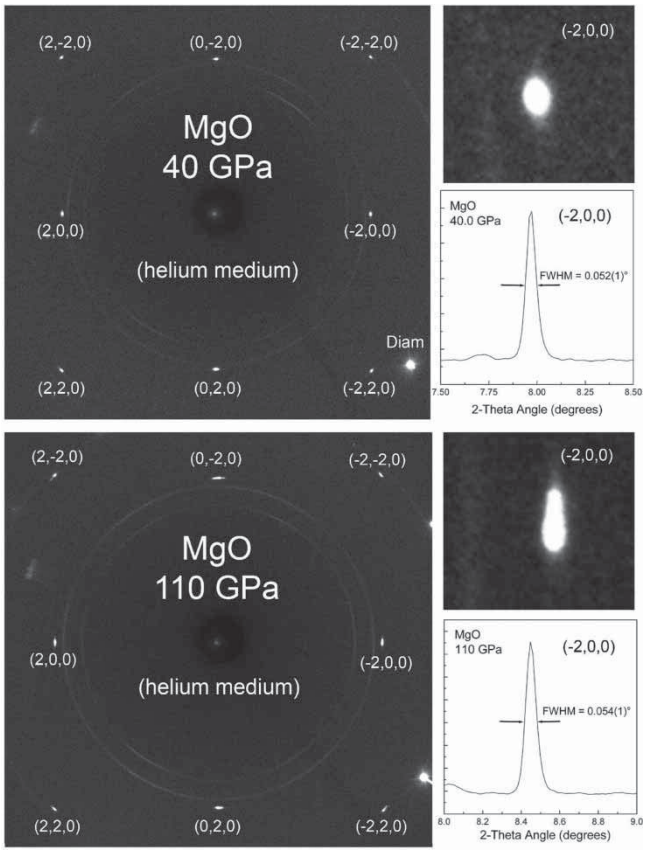

Figure 8. Diffraction patterns from single-crystal MgO in helium at 40 (top panel) and 110 GPa (lower panel) with monochromatic synchrotron X-radiation at 45 keV. The pattern is integrated over a ±7° oscillation in omega. Some diffraction rings from the rhenium gasket are also visible. Sharp diffraction spots measuring less than 0.06 degrees-2θ (FWHM) were maintained to the highest pressure.

image plate placed 450 mm from the sample. The diamond cell was fitted with cubic BN seat on the downstream side to widen the accessible angular aperture of the cell, which oscillated $\pm 7^\circ$ from the zero-omega position at a rate of about $0.25^\circ\ s^{-1}$ (60 s exposure). The geometry of the image plate was calibrated with a CeO_2 standard.

6.4. *Experimental results*

Diffraction patterns from the MgO crystal compressed in helium at 40 and 110 GPa are shown in Figure 8. Two classes of reflections were observed ($h00$ and $hk0$), resulting in eight reflection positions for cell-parameter fitting. Volumes were calculated using the UnitCell program of Holland and Redfern [20], a non-linear least-squares refinement program with regression diagnostics.

In order to demonstrate the difference between quasi-hydrostatic and non-hydrostatic conditions, we also obtained diffraction patterns of single-crystal MgO loaded in a solid KCl pressure medium, using otherwise the exact same procedure. Figure 9 shows diffraction patterns from MgO compressed in KCl at 7.4 and 80 GPa, illustrating how line broadening in 2θ, but especially in χ and ω (not shown), would adversely affect peak positioning, and therefore the precision of equation-of-state studies.

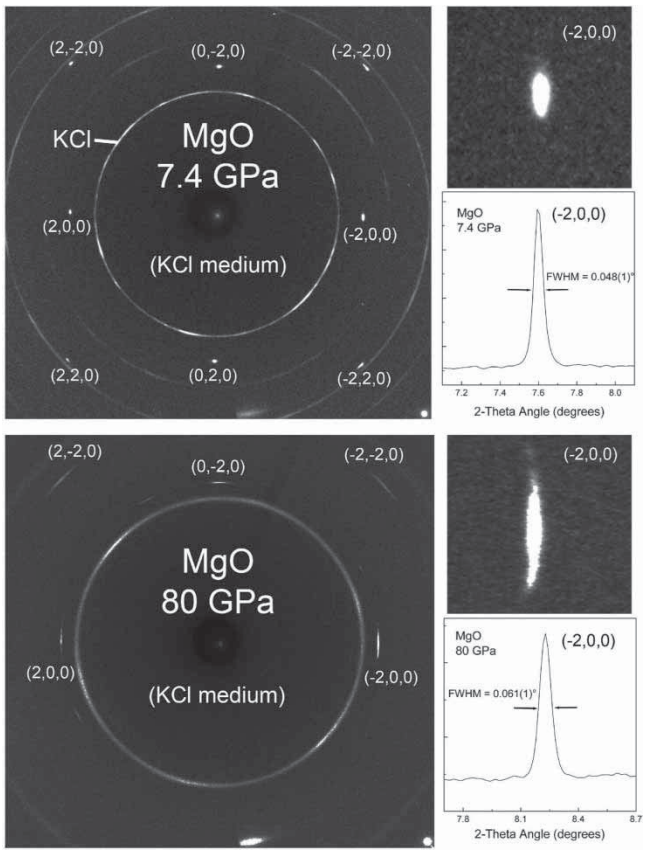

Figure 9. Diffraction patterns from single-crystal MgO in a non-hydrostatic KCl pressure medium helium at 7.4 (top panel) and 80 GPa (lower panel) with monochromatic synchrotron X-radiation at 45 keV. The pattern is integrated over a $\pm 10^\circ$ oscillation in omega. Some diffraction rings from the KCl pressure medium are also visible. Broadening of the diffraction spots in χ and ω (out of plane, not shown) is indicative of high stress conditions.

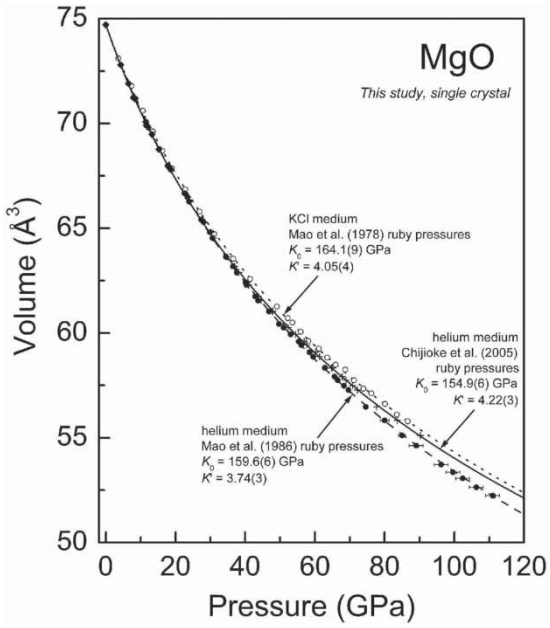

Figure 10. Static compression of single-crystal MgO in helium (filled circles) and in a non-hydrostatic KCl pressure medium (open circles). A third-order Birch–Murnaghan equation-of-state was fitted to the non-hydrostatic compression data using the non-hydrostatic ruby pressure gauge [24], shown by the short-dashed line, which is in good agreement with previous equations of state for MgO [10,11]. Two different quasi-hydrostatic ruby pressure gauges were used to evaluate the helium compression data, shown by the long-dashed line [25] and the solid line with plus symbols [26]. Discrepancies between these quasi-hydrostatic equations of state emphasize the need to evaluate ruby-fluorescence pressure gauges for helium media in the 50–100 GPa range [26–28].

The new compression data and fitted equations of state from the quasi-hydrostatic (helium) and non-hydrostatic (KCl) compression studies of MgO are shown in Figure 10. Because ruby spectra from the six highest pressures (>85 GPa) were not as reliable as lower pressures, diamond-Raman pressures [21] are plotted and those points are excluded in the following preliminary equation-of-state analysis. Fitting a third-order Birch–Murnaghan equation of state [22] to the non-hydrostatic (KCl medium) data yields $K_{T0} = 164.1(9)$ GPa for the isothermal bulk modulus (K_{T0}), and $K' = 4.05(4)$ for the pressure derivative of the bulk modulus ($K' = dK_T/dP$) using the non-hydrostatic ruby-fluorescence pressure scale of Mao et al. [23]. However, equation of state fitting to the MgO volumes obtained in helium (filled symbols in Figure 10) yields $K_{T0} = 159.6(6)$ GPa and $K' = 3.74(3)$ using the quasi-hydrostatic ruby pressure gauge of Mao et al. (1986) [24]. The difference in these two equations of state translates roughly to a difference in calculated pressure from the MgO volume of about 8 GPa at 100 GPa. Because the quasi-hydrostatic ruby pressure gauge [24] was calibrated using equations of state for Cu compressed in an Ar pressure medium, it is possible that a revised ruby pressure gauge is required for the softer helium medium in the 50–100 GPa pressure range [25,26]. Using the ruby calibration for helium from Chijioke et al. [25] with our most reliable ruby spectra (excluding the six highest pressures shown in Figure 10), we obtain equation-of-state parameters for MgO of $K_{T0} = 154.9(6)$ GPa and $K' = 4.22(3)$, shown by the solid line in Figure 10. Because neither of the helium data sets reproduces the primary MgO pressure scale of Zha et al. [9] obtained up to 55 GPa, with $K_{T0} = 160.2$ GPa and $K' = 4.03$, we will further analyze the new MgO compression data in helium with emphasis on revised ruby-pressure calibrations for helium pressure media in the 50–100 GPa range in a forthcoming paper [27].

7. Future plans

We expect to be able to accommodate several additional cell types in the next few months. With some minor modification to the current cell clamp, we will be able to load cells of the ETH design (50 mm diameter, 25 mm tall). We will build a new cell clamp to load panoramic DACs, and we are currently accepting and prioritizing requests to build cell clamps for other types of DAC. We are upgrading the system to be able to rapidly switch between He and Ne and to be able to conveniently use other gases as well. We are also actively pursuing finding a vendor who can supply copies of this system commercially, since at least six other laboratories have expressed an interest in obtaining one.

Acknowledgements

The authors thank S. Sinogeikin for useful discussion, and N. Lazarz, F. Sopron, E. LaRue and G. Macha for technical support. Mati Meron helped with the safety analysis, and P.Dera was very helpful in commissioning of the system. This research was partially supported by COMPRES, the Consortium for Materials Properties Research in Earth Sciences under NSF Cooperative Agreement EAR 06-49658. It was also supported by GeoSoilEnviroCARS (Sector 13), Advanced Photon Source (APS), Argonne National Laboratory. GeoSoilEnviroCARS is supported by the National Science Foundation - Earth Sciences (EAR-0622171) and Department of Energy - Geosciences (DE-FG02-94ER14466). S.D. Jacobsen and C.M. Holl are supported in part by NSF EAR-0721449. Use of the Advanced Photon Source was supported by the U.S. Department of Energy, Office of Science, Office of Basic Energy Sciences, under Contract No. DE-AC02-06CH11357.

References

[1] A. Jephcoat, H. Mao, and P. Bell, *Static compression of iron to 78 GPa with rare gas solids as pressure-transmitting media*, J. Geophys. Res. 91 (1986), pp. 4677–4684.
[2] J. Thomasson, C. Ayache, I.L. Spain, and M. Villedieu, *Is $T_c(P)$ for lead suitable as a low-temperature manometer?* J. Appl. Phys. 68 (1990), p. 5933.
[3] R.L. Mills, D.H. Liebenberg, J.C. Bronson, and L.C. Schmidt, *Procedure for loading diamond cells with high-pressure gas*, Rev. Sci. Instrum. 51 (1980), pp. 891–895.
[4] T. Yagi, H. Yusa, and M. Yamakata, *An apparatus to load gaseous materials to the diamond-anvil cell*, Rev. Sci. Instrum. 67 (1996), pp. 2981–2984.
[5] T. Kenichi, P.Ch. Sahu, K. Yoshiyasu, and T. Yasuo, *Versatile gas-loading system for diamond-anvil cells*, Rev. Sci. Instrum. 72 (2001), pp. 3873–3876.
[6] B. Couzinet, N. Dahan, G. Hamel, and J.-C. Chervin, *Optically monitored high-pressure gas loading apparatus for diamond anvil cells*, High Press. Res. 23 (2003), pp. 409–415.
[7] H.-K. Mao, P. Bell, J. Shaner, and D. Steinberg, *Specific volume measurements of Cu, Mo, Pd, and Ag and calibration of the ruby R_1 fluorescence pressure gauge from 0.06 to 1 Mbar*, J. Appl. Phys. 49 (1978), p. 3276.
[8] T.S. Duffy, R.J. Hemley, and H.K. Mao, *Equation of state and shear strength at multimegabar pressures: Magnesium Oxide to 227 GPa*, Phys. Rev. Lett. 74 (1995), pp. 1371–1374.
[9] C.S. Zha, H.K. Mao, and R.J. Hemley, *Elasticity of MgO and a primary pressure scale to 55 GPa*, Proc. Natl Acad. Sci. USA 97 (2000), pp. 13494–13499.
[10] S. Speziale, C.S. Zha, T.S. Duffy, R.J. Hemley, and H.K. Mao, *Quasi-hydrostatic compression of magnesium oxide to 52 GPa: Implications for the pressure-volume-temperature equation of state*, J. Geophys. Res. 106 (2001), pp. 515–528.
[11] Y. Fei, J. Li, K. Hirose, W. Minarik, J. Van Orman, C. Sanloup, W. van Westrenen, T. Komabayashi, and K.I. Funakoshi, *A critical evaluation of pressure scales at high temperatures by in situ X-ray diffraction measurements*, Phys. Earth. Planet. Int. 143 (2004), pp. 515–526.
[12] H. Spetzler, *Equation of state of polycrystalline and single-crystal MgO to 8 kilobars and 800 K*, J. Geophys. Res. 75 (1970), pp. 2073–2087.
[13] G.L. Chen, R.C. Liebermann, and D.J. Weidner, *Elasticity of single-crystal MgO to 8 gigapascals and 1600 kelvin*, Science 280 (1998), pp. 1913–1916.
[14] S.D. Jacobsen, H.J. Reichmann, H.A. Spetzler, S.J. Mackwell, J.R. Smyth, R.J. Angel, and C.A. McCammon, *Structure and elasticity of single-crystal (Mg, Fe)O and a new method of generating shear waves for gigahertz ultrasonic interferometry*, J. Geophys. Res. 107 (2002), p. 2037, doi: 10/1029/2001JB000490.
[15] S.V. Sinogeikin, D.L. Lakshtanov, J.D. Nicholas, and J.D. Bass, *Sound velocity measurements on laser-heated MgO and $Al2O_3$*, Phys. Earth Planet Int. 143 (2004), pp. 575–586.
[16] B.B. Karki, R.M. Wentzcovitch, S. de Gironcoli, and S. Baroni, *First-principles determination of elastic anisotropy and wave velocities of MgO at lower mantle conditions*, Science 286 (1999), pp. 1705–1707.

[17] P. Dera, C.T. Prewitt, and S.D. Jacobsen, *Structure determination by single-crystal X-ray diffraction (XRD) at megabar pressures*, J. Synchr. Rad. 12 (2005), pp. 547–548.
[18] S.D. Jacobsen, J.F. Lin, R.J. Angel, G. Shen, V.B. Prakapenka, P. Dera, H.K. Mao, and R.J. Hemley, *Single-crystal synchrotron X-ray diffraction study of wüstite and magnesiowüstite at lower-mantle pressures*, J. Synchr. Rad. 12 (2005), pp. 577–583.
[19] H.K. Mao, R.J. Hemley, Y. Wu, A.P. Jephcoat, L.W. Finger, C.S. Zha, and W.A. Bassett, *High-pressure phase diagram and equation of state of solid helium from single-crystal X-ray diffraction to 23.3 GPa*, Phys. Rev. Lett. 60 (1988), pp. 2649–2652.
[20] T.J.B. Holland and S.A. Redfern, *Unit-cell refinement from powder diffraction data: the use of regression diagnostics*, Min. Mag. 61 (1997), pp. 65–67.
[21] L. Sun, A.L. Ruoff, and G. Stupian, *Convenient optical pressure gauge for multimegabar pressures calibrated to 300 GPa*, Appl. Phys. Lett. 86 (2005), p. 014103.
[22] R.J. Angel, *Equations of state*, Rev. Min. Geochem. 41 (2000), pp. 35–59.
[23] H.K. Mao, P.M. Bell, J. Shaner, and D. Steinberg, *Specific volume measurements of Cu, Mo, Pd, and Ag and calibration of the ruby R_1 fluoresence pressure gauge from 0.06 to 1 Mbar*, J. Appl. Phys. 49 (1978), pp. 3276–3283.
[24] H.K. Mao, J. Xu, and P.M. Bell, *Calibration of the ruby pressure gauge to 800 kbar under quasi-hydrostatic conditions*, J. Geophys. Res. 91 (1986), pp. 4673–4676.
[25] A.D. Chijioke, W.J. Nellis, A. Soldatov, and I.F. Silvera, *The ruby pressure standard to 150 GPa*, J. Appl. Phys. 98 (2005), p. 114905.
[26] A. Dewaele, P. Loubeyre, and M. Mezouar, *Equations of state of six metals above 94 GPa*, Phys. Rev. B 70 (2004), p. 094112.
[27] S.D. Jacobsen, C.M. Holl, K.A. Adams, R.A. Fischer, E.S. Martin, C.R. Bina, J.F. Lin, V.B. Prakapenka, A. Kubo, and P. Dera, *Compression of single-crystal magnesium oxide to 118 GPa and a ruby pressure gauge for helium pressure media*, Am. Mineral. 93, DOI: 10.2138/am.2008.2988.
[28] K. Tanaka, M. Mishida, and N. Takada, *High-speed penetration of a projectile into aluminum alloys at low temperatures*, Int. J. Impact Eng. 33 (2006), pp. 788–798.